Assessment of Pulmonary Lesions with ^{18}F-Fluorodeoxyglucose Positron Imaging Using Coincidence Mode Gamma Cameras

Wolfgang Weber, Carter Young, Hussein M. Abdel-Dayem, George Sfakianakis, G. John Weir, Charles M. Swaney, Mark Gates, Marcel P. Stokkel, Anthony Parker, Horace Hines, Behrouz Khanvali, John R. Liebig, Ann N. Leung, Richard Sollitto, Gary Caputo and Henry N. Wagner, Jr.

Technical University Munich, Munich, Germany; Methodist Medical Center, Peoria, Illinois; St. Vincents, New York, New York; University of Miami, Miami, Florida; Marshfield Clinic & St. Joseph's Hospital, Marshfield, Wisconsin; Boone Hospital Center, Columbia; Southeast Missouri Hospital, Cape Girardeau, Missouri; Utrecht University Hospital, Utrecht, Holland; Beth Israel Deaconess Medical Center, Boston, Massachusetts; ADAC Laboratories, Milpitas; Stanford University Medical Center, Stanford; University of California, San Francisco, California; Johns Hopkins Medical Institutions, Baltimore, Maryland

Accurate assessment of lung carcinoma remains a significant clinical problem, often leading to surgical procedures without curative potential. PET with ^{18}F-fluorodeoxyglucose (FDG) has shown promise in differentiating benign from malignant lesions and in staging the extent of disease, resulting in improved treatment at a significant cost savings. This multicenter prospective study used dual-detector coincidence imaging with FDG to categorize pulmonary lesions as benign or malignant. The goal of this study was to determine the sensitivity and specificity of dual-detector coincidence imaging of FDG in patients with pulmonary lesions who were scheduled to have a diagnostic procedure for histopathologic confirmation. **Methods:** A total of 96 patients with pulmonary lesions with a lesion size ranging from 1 to 7 cm with a mean of 3.44 cm based on their chest radiograph or CT scan were studied using FDG scans with a dual-detector coincidence detection system. An additional 24 patients were entered as control subjects. The studies of 120 subjects were interpreted in random order by three physicians experienced in the use of FDG in patients with lung cancer. Surgical pathology was used as the standard for identifying malignant lesions. **Results:** There was 94% agreement between the readers in the independent interpretation of the FDG studies. In the 96 patients with pulmonary lesions, FDG studies were 97% sensitive and 80% specific in identifying proven malignant lesions. **Conclusion:** The results of this prospective study provide evidence that dual-detector coincidence imaging with FDG provides an accurate, sensitive and specific means of diagnosing malignancy in patients with pulmonary lesions.

Key Words: solitary pulmonary lesions; ^{18}F-fluorodeoxyglucose; dual-detector coincidence imaging

J Nucl Med 1999; 40:574–578

Lung cancer continues to be a significant worldwide health problem with nearly 200,000 new cases reported in the U.S. every year (*1*). The initial lesion in patients with lung cancer is usually detected by chest radiography performed because of respiratory symptoms, during a routine annual examination or preoperatively in patients undergoing surgery for some other disease. The next step is to determine whether the chest lesion is benign or malignant. In patients 35 y old or older, at least one third of such chest lesions will be malignant, either as primary lung cancer or as metastatic disease to the lung from another organ system (*2*). In patients who smoke, the risk of cancer is four times higher than in nonsmokers. In younger persons, the risk of cancer is much less. Presently, the gold standard is histopathologic diagnosis. Biopsies with fluoroscopic, bronchoscopic or CT guidance are performed on lesions. Percutaneous biopsy has an 18%–24% risk of a complication, such as pneumothorax, requiring chest tube placement and hospitalization (*3*).

Several reports have suggested that the use of ^{18}F-fluorodeoxyglucose (FDG) positron imaging may enhance diagnostic accuracy and significantly reduce cost and morbidity in this patient population. Previous studies performed throughout the world have used FDG and PET to aid in the diagnosis and staging of lung cancer (*4–13*).

Positron imaging is usually performed with "dedicated" (with "dedicated" meaning systems able to detect only the 511-keV photons emitted by positron emitting tracers) PET scanners that use a full ring of detectors. Recently, Muehllehner et al. (*14*) reported a modification of a dual-detector SPECT system to enable operation in "coincidence" mode. The modified system is capable of operating in coincidence mode as well as imaging lower-energy photons, such as the 140 keV of ^{99m}Tc. As part of the initial clinical evaluation of a hybrid dual-detector gamma camera operated in coincidence mode, a prospective multicenter trial was designed to

Received Apr. 17, 1998; revision accepted Oct. 1, 1998.

For correspondence or reprints contact: Henry N. Wagner, Jr., MD, Johns Hopkins Medical Institutions, Divisions of Nuclear Medicine and Radiation Health Sciences, 615 N. Wolfe St., Baltimore, MD 21205–2179.

assess the diagnostic accuracy of FDG dual-detector coincidence imaging in the diagnosis of pulmonary lesions.

MATERIALS AND METHODS

Because the study was designed as an initial evaluation of coincidence imaging, wide inclusion criteria were used: All patients who were scheduled to undergo surgery for an intrapulmonary lesion detected by chest radiography or CT were eligible. The inclusion criteria did not specify a size range.

Patient Selection

Inclusion criteria included the presence of a pulmonary lesion as seen on chest radiography or CT with subsequent histopathologic verification of diagnosis either by resection or biopsy. The lesion size range was 1.0–7.0 cm with a mean of 3.44 cm. Ninety-six patients were studied (66 men, average age 63.9 y, range 36–95 y; 30 women, average 61.9 y, range 36–82 y). There were 86 malignant cases all verified by histopathology (surgical removal in 71 cases, biopsy in 15 cases). Eight of the 10 benign cases were verified by histopathology (surgical removal in 5, needle biopsy in 3). In 2 patients, follow-up examinations compared with previous CT studies showed no changes over a period >1 y. Therefore, these patients were not operated on but observed further. The histological tumor types were adenocarcinoma (n = 44), squamous cell carcinoma (n = 30), small cell carcinoma (n = 4), large cell carcinoma (n = 3), neuroendocrine carcinoma (n = 2), metastatic melanoma (n = 2) and bronchiolo-alveolar carcinoma (n = 1).

Twenty-four additional subjects without lung disease served as controls. Because the inclusion criteria resulted in a pretest bias to malignancy, control subjects were introduced into the study population to reduce any selection bias the inclusion criteria may have created. The interpreters were completely blinded to the prevalence of disease.

Patient Preparation

All patients participating in the study gave informed consent to a protocol approved by the facility's institutional review board. After fasting for at least 4 h, all patients and control subjects were administered FDG by intravenous injection. Physical activity was limited to minimize muscle uptake of FDG. Patients examined with dual-detector coincidence systems received only 185 MBq (5 mCi) FDG and were imaged at 1 h postinjection. Blood glucose levels were not monitored before acquisition start, and the relationship between blood sugar and tumor uptake was not evaluated in this series. Patients examined at institutions with both dedicated PET and dual-detector coincidence systems received 370 MBq (10 mCi) FDG and were imaged with dual-detector coincidence imaging at 2.5 h postinjection.

Technical Performance

All patient studies were acquired on a dual-detector gamma camera (Vertex Molecular Coincidence Detection; ADAC Laboratories, Milpitas, CA) equipped with a 5/8-in. (1.5-cm) crystal that was placed into coincidence mode for acquisition. All patients were imaged for 32 stops through a rotation of 180° per detector at 40 s/frame for a total acquisition time of approximately 23 min per patient bed position. The data were acquired in three-dimensional mode, and decay correction was performed during the acquisition. Patients were imaged over the entire thorax and scanned for one or two bed positions, depending on the size of the patient. The axial field of view was 38 cm when one bed position was used (n = 23) and 57 cm when two bed positions were used (n = 97). Images were not corrected for photon attenuation. The coincidence mode of acquisition used all photopeak-photopeak events as well as the photopeak-Compton scatter events. No Compton-Compton counts were accepted. The energy windows were set at 511 keV/30% for the ^{18}F photopeak and 310 keV/30% for the Compton events in the NaI crystal. The range of singles counting rates for patients enrolled in the study was 500,000–2,000,000 counts/s, which included both windowed and unwindowed events. The observed total coincidence counting rate was ≤30,000 Hz, which includes true, random and scattered events. The performance of the dual-detector coincidence system was measured to have a sensitivity of 100 kcps/μCi/mL and a maximum true counting rate of 13,800 Hz using the North American Equipment Manufacturers Association phantom and protocol. The total counts in the projection data ranged from 20 to 35 million counts for each bed position. The detectors have a timing resolution of 6 ns, and a 15-ns timing window was used to acquire the coincidence events.

Reconstruction of Images

Each dataset was rebinned using single-slice rebinning and then reconstructed using an ordered subset expectation maximization iterative algorithm (*15*). The parameters used to perform the iterative reconstruction included an ordered subset of eight with a Wiener prefilter and a noise factor of 0.7 (*16*) with two iterations. No attenuation or random correction techniques were used in this study. The images were reconstructed into a 128 × 128 × 128 volume of 4-mm cubic voxels.

CT was performed using modern CT scanners in the same institution as the positron imaging. Acquisition parameters and the use of intravenous contrast agents were at the discretion of the supervising physician.

Interpretation of Images

Qualitative interpretation of the studies was performed independently by three nuclear medicine physicians with at least 5 y of experience in interpreting dedicated FDG PET oncology studies. Two of the three interpreters had no previous experience with dual-detector coincidence studies. The first reader interpreted all 120 cases. The second reader viewed the first 18 malignant cases, 1 benign and 7 controls. The third reader read the remaining 68 malignant cases, 9 benign cases and all 24 controls. During interobserver comparison, the results of the second and the third readers were combined and presented as one interpreter. Readers were asked to score the study for the presence of lung cancer (yes or no) and the percent certainty of diagnosis (0%–100%). The images were interpreted twice; first with only FDG images and then with the accompanying CT images of the chest and upper abdominal areas.

A separate blinded reading was also performed on the CT scans by two chest radiologists. The CT studies were interpreted in random order and were scored regarding the size of the lesion and location. The coincidence images were interpreted independently by the physicians in separate rooms. The coronal images were reviewed first (Fig. 1) followed by transaxial and sagittal images all in 4-mm slices. After systematic viewing of the three orthogonal planes, the reader viewed a three-dimensional volume display of the data and was able to simultaneously triangulate corresponding regions on the orthogonal views. The images were displayed using a gray scale (white on black) in which maximum activity was shown as white, with automatic scaling of the images with the highest pixel count being shown as maximum whiteness. The

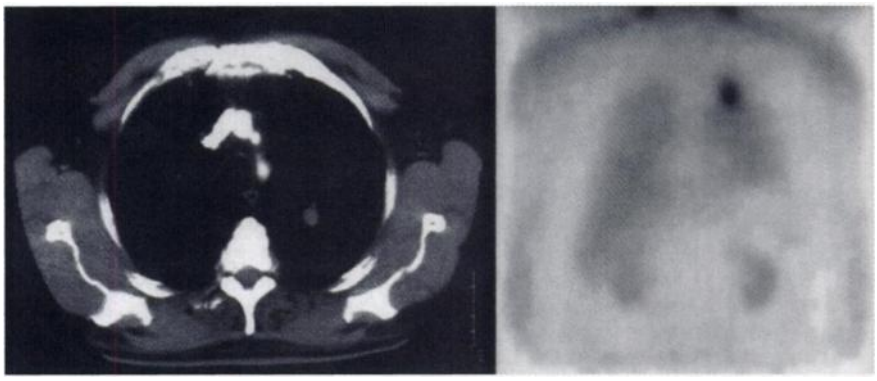

FIGURE 1. (Left) Coronal view of 1.5-cm solitary pulmonary lesion in left lobe of lung. (Right) Coronal view of same lesion with FDG coincidence detection.

interpretations of the FDG images were made from the computer screen without the use of film. After the standard presentation of the images, the reader was allowed to adjust the scaling of the images to his personal preference and view the images in any desired order. A study was scored as positive by visual interpretation when discrete focal uptake greater than background (with a target-to-background ratio >2.5:1) was identified in the lung. The statistical analysis calculations of sensitivity and specificity of FDG imaging and CT, interpreted independently, were derived using standard formulas.

Quantitative Analysis

In 39 patients with malignant lesions (size 3.7 ± 1.5 cm, range 1–7 cm), a quantitative analysis of lesion contrast was performed. The maximum counting rate within the tumors was determined (tu_{max}). A large region of interest in the contralateral normal lung was used as a refererence structure. Lesion contrast was expressed as maximum counting rate within the tumor divided by the mean counting rate in normal lung (ref). Furthermore, a signal-to-noise ratio defined as (tu_{max} − ref) / SD(ref) was calculated.

The statistical analysis calculations of sensitivity and specificity of FDG imaging were derived using standard formulas. Kappa statistics were used to describe the agreement of two observers in the interpretation of the FDG studies. To assess differences in sensitivity and specificity between groups of patients, Fisher exact test was applied. Linear regression analysis and the Kruskal-Wallis test were used to analyze the influence of lesion size on image contrast.

RESULTS

There was 94% agreement (113/120, $\kappa = 0.862$; $P < 0.01$) among interpreters in the FDG-only image interpretations. The three readers correctly diagnosed 82 of 86, 18 of 18 and 61 of 68 of the malignant lesions, respectively. The overall sensitivity was 97% (using the consensus read to categorize discordant cases). In 5 patients with lung disease about whom the two readers disagreed, a third reader was used to categorize the interpretation of the study. The average levels of certainty reported by each of the readers in the malignant cases were 97% for reader 1, 97% for reader 2 and 92% for reader 3. The level of certainty of the observers in their diagnosis did not show an association with the histological tumor type. There were 3 false-negatives in patients with malignancies; that is, the lesions were interpreted as probably benign.

In the case of benign lesions, the three readers correctly interpreted 8 of 10, 0 of 1 and 8 of 9, respectively, giving an overall specificity of 80%. The average levels of certainty reported by each of the readers in the benign cases was 93% for reader 1, 95% for reader 2 and 64% for reader 3. The 2 false-positive cases were determined to be tuberculosis and nonspecific inflammatory disease. There were no FDG studies deemed inadequate by any of the interpreters

In the control subjects, two readers interpreted 24 FDG studies in patients without lung disease. The first reader interpreted 92% (22/24) correctly. In the 2 false-positive cases, diffuse uptake was misinterpreted. In the first case, diffuse uptake in the liver was incorrectly interpreted. In the second case, diffuse uptake in the lower right lung was interpreted as positive. The second and third reader interpreted 100% (24/24 and 7/7, respectively) of the control studies correctly.

Comparing the size of the lesion (Fig. 2) versus sensitivity of FDG dual-detector coincidence imaging, the lesions were categorized into three groups. Lesions in the first group were

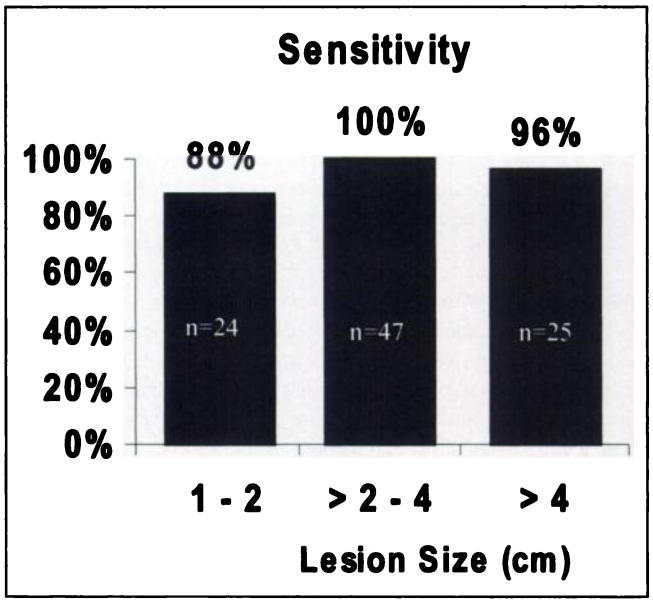

FIGURE 2. Sensitivity as function of lesion size.

≤2 cm (n = 24) with an average size of 1.61 cm and SD of 0.39 cm. Lesions in the second group were >2 cm and ≤4 cm (n = 47) with an average size of 3.21 cm and SD of 0.57 cm. Lesions in the third group were >4 cm (n = 25) with an average size of 5.65 cm and SD of 0.73 cm. The sensitivity values of the three groups were 88%, 100% and 96%, respectively. The sensitivity in the smallest group was less than the sensitivity in the two larger groups. This difference was not statistically significant (Fisher exact test = 4.634; $P = 0.058$). Specificities were 85%, 50% and 100% for the three respective size categories. There were no statistically significant differences in these values, due to the small number of benign cases (n = 10).

Quantitative analysis revealed a lesion contrast of 4.2 ± 2. The signal-to-noise ratio was 34 ± 24. There was a statistically significant trend for decreased contrast with decreasing lesion size ($r = 0.44$; $P = 0.0053$ by linear regression analysis). For lesions with a diameter of 1–2, 2–4 and >4 cm, the contrast was 3.1 ± 2.4, 3.6 ± 1.4 and 5.9 ± 2.7, respectively ($P = 0.01$, Kruskal-Wallis test, Fig. 3).

There were 86 malignant cases verified by histopathology as adenocarcinoma (n = 44), squamous cell carcinoma (n = 30), small cell carcinoma (n = 4), large cell carcinoma (n = 3), neuroendocrine carcinoma (n = 2), bronchiolo-alveolar carcinoma (n = 1) and metastatic melanoma (n = 2).

When CT scans were included in the reading process, the interpretation was altered in 1 patient. A 5-cm lesion with a necrotic center in the left lower lobe of the lung was incorrectly interpreted with only FDG as normal cardiac activity. When the CT scan was introduced, the interpretation was correctly changed to malignant.

CT was performed in 93 of the 96 (97%) patients with histologically proven benign and malignant disease. The control subjects did not undergo this examination. Eighty-eight of 93 (95%) CT examinations were considered technically adequate by the first CT reader. The second reader interpreted 85 of 93 (92%) scans. The first CT reader was 99% (79/80) sensitive and 38% (3/8) specific. Reader two was 100% (78/78) sensitive and 29% (2/7) specific. The CT scans were used to size and locate the lesions. Three CT scans could not be obtained for interpretation and entry into this study; 2 benign and 1 malignant case. The inadequate examinations occurred in 5 malignant cases for reader 1 and in 1 benign and 7 malignant cases for reader 2. The examinations were considered inadequate because they did not include the entire lung and mediastinal windows. In these 3 cases, the size of the lesion was determined from the histopathologic specimen.

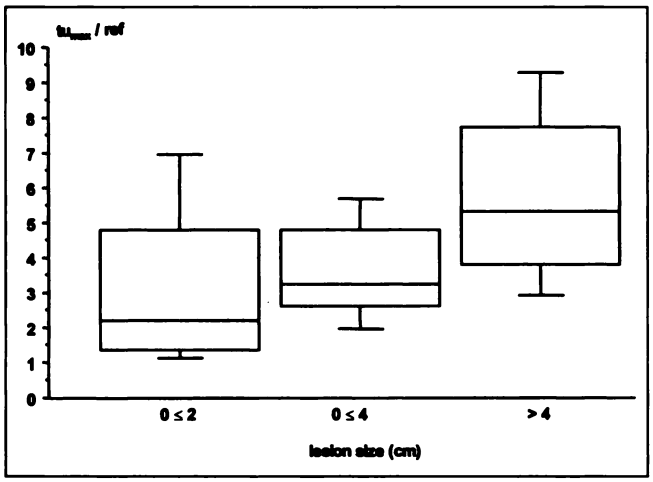

FIGURE 3. Box diagram shows influence of lesion size on image contrast. Whiskers denote 1SD; boxes denote 25% and 75% percentiles. Contrast increases significantly with increasing lesion size (Kruskal-Wallis test, $P = 0.01$).

DISCUSSION

This prospective study demonstrates that dual-detector coincidence imaging with FDG with a gamma camera operated in coincidence mode provides an accurate means for differentiating between benign and malignant pulmonary lesions. In the 96 patients with lung disease, there was an overall sensitivity of 97% and a specificity of 80% was achieved. A quantitative analysis of the image data showed that malignant lesions were generally imaged with a high tumor-to-background ratio of approximately 4:1.

The false-positive cases in these patients were due to inflammatory processes (tuberculosis and nonspecific inflammatory disease). Several previous reports using dedicated PET systems have demonstrated that localized uptake of FDG in active inflammation is a common cause of false-positive findings (*10*).

There were 3 false-negative studies. The first was a 1-cm metastatic melanoma lesion in the lateral aspect of the left upper lobe. The second was a 1-cm papillary adenocarcinoma in the lateral aspect of the right upper lobe. The third was a 5.5-cm bronchiolo-alveolar carcinoma in the right upper lobe. Bronchiolo-alveolar carcinomas are a known cause for false-negative FDG studies. Often, even large tumors are not visualized. In a recent study using a dedicated PET system, the FDG uptake in bronchiolo-alveolar carcinomas was only one third of other adenocarcinomas (*17*).

Because of partial-volume effects, the contrast between tumor and normal lung decreased significantly with decreasing lesion size. Accordingly, there was a trend toward reduced sensitivity for smaller lesions that was 88% for lesions <2 cm versus 98% for lesions >2 cm. The Fisher exact test showed that this trend was not significant at the 5% level ($P = 0.058$). The high signal-to-noise ratio of the images indicates that it may be possible to reconstruct the coincidence studies with less smoothing. In the future, this may improve the image contrast and the detectability of small lesions.

The prevalence of malignant lesions in this study is clearly higher than in previous studies using dedicated PET systems for the evaluation of solitary pulmonary lesions (*10*). In these studies, the prevalence of lung cancer or other malignant tumors generally ranges between 40% and 60%. However, in this study all types of pulmonary lesions were

included when the patient was scheduled for biopsy or surgery. Therefore, lung cancer presenting in any form was studied. Consequently, the number of malignant cases in this study is higher. Because only patients scheduled to undergo surgery or biopsy were included, this may have increased the number of patients with malignant disease.

Because of the small number of patients with benign lesions, the specificity of coincidence imaging determined in this study has to be interpreted with caution. Although the control subjects are not a substitute for patients with benign pulmonary lesions, they demonstrate that coincidence images did not show artifacts that cause false-positive image interpretations. This suggests that the specificity of coincidence imaging for evaluation of pulmonary lesions may be comparable with a dedicated PET system.

The mean diameter of the lesions in this study is 3.4 cm, which is somewhat larger than in previous studies in solitary pulmonary lesions (*10*). The larger lesion diameter in this study is probably due to two factors. First, malignant pulmonary lesions generally have a larger diameter than benign nodules. Because the prevalence of malignant lesions in this study was high, this has consequently increased the lesion diameter. Second, the definition of a solitary pulmonary lesion directly or indirectly imposes some restriction on the size of the lesion. This study included all forms of pulmonary lesions without a restriction on size and this may have also increased the diameter of the lesions.

Because of the high prevalence of malignant lesions, a direct comparison between the results of this study and published data for dedicated PET systems (*4–13*) is difficult. The patients enrolled in this study had a high prevalance of malignancy because they were selected based on ensuing surgery to prove the diagnosis. When the probability of malignancy was lower, the patients were observed and not operated on. Therefore, they were not eligible. However, based on this fact, the present findings suggest that a coincidence gamma camera provides a similar sensitivity for detection of malignant pulmonary lesions with a diameter >2 cm to that of dedicated PET systems (*4–13*). Furthermore, the high agreement between observers in the interpretation of FDG examinations (94%) and the low number of false-positive results in the control subjects suggest that the specificity may be comparable with dedicated systems.

The prevalence of malignant lesions in this study is clearly higher than in previous studies using dedicated PET systems for the evaluation of solitary pulmonary nodules. In these studies the prevalence of lung cancer or other malignant tumors generally ranges between 40% and 60%. However, in this study all types of pulmonary lesions were included. Therefore, lung cancer presenting in any form was studied. Consequently, the number of malignant cases in this study increased. Furthermore, only patients scheduled to undergo surgery were included, thereby increasing the number of patients with malignant disease.

CT detects pulmonary paranchymal disease with high sensitivity because of the excellent anatomic resolution of the modality, and these results confirm this fact with a sensitivity of 99%. However, the specificity of the CT interpretations for benign disease in this study was 33% (3/8 and 2/7) with a confidence interval from 9% to 75% due to the small number of subjects. Additionally, CT data were collected from multiple institutions some of which used helical CT, with variations in CT technology. It should be noted that the specificity for CT in the literature is approximately 60%. The lower specificity in this study can be explained by the small number of benign cases, which results in a wide confidence interval in this series. When taking the confidence level into consideration, the findings in this study are consistent with the published literature (*18*).

CONCLUSION

The results of this prospective study provide evidence that dual-detector coincidence imaging with FDG by scintillation cameras provides a useful test in the diagnosis of malignancy in patients with pulmonary lesions.

REFERENCES

1. Beckett WS. Epidemiology and etiology of lung cancer. *Clin Chest Med.* 1993;14:1–15.
2. Khouri NF, Meziane MA, Zerhouni EA, Fishman EK, Siegelman SS. The solitary pulmonary nodule assessment, diagnosis and management. *Chest.* 1987;91:128–133.
3. Dewan NA, Reeb SD, Gupta NC, Gobar LS, Scott WJ. PET-FDG imaging and transthoracic needle lung aspiration biopsy in evaluation of pulmonary lesions. *Chest.* 1995;108:441–446.
4. Dewan NA, Gupta NC, Redepenning LS, Phalen JJ, Frick MP. Diagnostic efficacy of PET-FDG imaging in solitary pulmonary lesions. *Chest.* 1993;104:997–1002.
5. Ishiwata K, Takahashi T, Iwata R, et al. Tumor diagnosis by PET: potential of seven tracers examined in five experimental tumors including an artificial metastasis model. *Int J Radiat Appl Instru (B).* 1992;19:611–618.
6. Kubota K, Matsuzawa T, Fujiwara T, et al. Differential diagnosis of lung tumor with positron emission tomography: a prospective study. *J Nucl Med.* 1990;31: 1927–1932.
7. Kubota K, Yamada S, Ishiwata K, Ito M, Ido T. Positron emission tomography for treatment evaluation and recurrence detection compared with CT in long-term follow-up cases of lung cancer. *Clin Nucl Med.* 1992;17:877–881.
8. Nolop KB, Rhodes CG, Brudin LH, et al. Glucose utilization in vivo by human pulmonary neoplasms. *Cancer.* 1987;60:2682–2689.
9. Patz E, Lowe VJ, Hoffman JM, Paine S, Harris L, Goodman PC. Detection of persistent or recurrent bronchogenic carcinoma using ^{18}F-2-Deoxy-D-glucose and positron emission tomography (PET) imaging [abstract]. *Radiology.* 1993;89:147.
10. Patz EF, Lowe VJ, Hoffman JM, et al. Evaluation of pulmonary abnormalcontrolities with ^{18}F-2-fluoro-2-deoxy-D-glucose and positron emission tomography (PET) imaging. *Radiology.* 1993;188:487–490.
11. Rege SD, Hoh CK, Glaspy JA, et al. Imaging of pulmonary mass lesions with whole-body positron emission tomography and fluorodeoxyglucose. *Cancer.* 1993;72:82–90.
12. Strauss LG, Conti PS. The applications of PET in clinical oncology. *J Nucl Med.* 1991;32:623–648.
13. Lowe VJ, Fletcher JW, Gobar L, et al. Prospective investigation of positron emission tomography in lung nodules. *J Clin Oncol.* 1998;16:1075–1084.
14. Muehllehner G, Geagan M, Countryman P, Nellemann P. SPECT scanner with PET coincidence capability [abstract]. *J Nucl Med.* 1995;36:70P.
15. Hudson HM, Larkin RS. Accelerated image reconstruction using ordered subsets of projection data. *IEEE Trans Med Imaging.* 1994;13:601–609.
16. Shao L. Practical considerations of wiener filter technique on projection data for PET. *IEEE Trans Nucl Sci.* 1994;41:1560–1565.
17. Kim BT, Kim Y, Lee KS, et al. Localized form of bronchioloalveolar carcinoma: FDG PET findings. *AJR.* 1998;170:935–939.
18. Siegelman SS, Khouri NF, Leo FP, Fishman EK, Braverman RM, Zerhouni EA. Solitary pulmonary nodules: CT assessment. *Radiology.* 1986;160:307–312.